

## Heavy quarkonium spectroscopy in pNRQCD with lattice QCD input

---

**Yoshiaki Koma**<sup>\*†</sup>

*Numazu College of Technology*

*E-mail: koma@numazu-ct.ac.jp*

**Miho Koma**<sup>‡</sup>

*Numazu College of Technology*

*E-mail: m-koma@numazu-ct.ac.jp*

The charmonium and bottomonium mass spectra are investigated in potential nonrelativistic QCD (pNRQCD) with the heavy quark potential computed by lattice QCD simulations. The potential consists of a static potential and relativistic corrections classified in powers of the inverse of heavy quark mass  $m$ , and the effects of the  $O(1/m)$  and  $O(1/m^2)$  spin-orbit corrections on the mass spectra are examined systematically. The pattern of the mass spectra is found to be in fairly good agreement with experimental data, in which the  $O(1/m)$  correction gives an important contribution.

*The 30th International Symposium on Lattice Field Theory*

*June 24 - 29, 2012*

*Cairns, Australia*

---

<sup>\*</sup>Speaker.

<sup>†</sup>Y.K. is partially supported by the Ministry of Education, Science, Sports and Culture, Japan, Grant-in-Aid for Young Scientists (B) (24740176).

<sup>‡</sup>M.K. is supported by Japan Society for the Promotion of Science (JSPS), Grant-in-Aid for JSPS Fellows (20-40152).

## 1. Introduction

It is of great challenge to understand a systematic pattern of heavy quarkonium mass spectra [1] from nonperturbative QCD. Lattice QCD simulations offer strong tools to gain an understanding of nonperturbative QCD, which enable us to compute the mass spectra of quarkonia directly by evaluating appropriate correlation functions of operators on the lattice. However, due to a hierarchical mixture of ultraviolet and infrared physics in the quarkonium system, it is not straightforward to deduce the underlying mechanism responsible for the mass spectra from the conventional simulation results.

One way to solve the hierarchical problem in the quarkonium system is to employ effective field theories (EFTs). In this context, the use of nonrelativistic QCD (NRQCD) [2, 3] and potential NRQCD (pNRQCD) [4, 5, 6] have been proposed. The aim of EFTs is generally to have better control of a hierarchy of energy scales in an original theory for a high precision calculation. For instance, suppose there exist two typical energy scales which satisfy  $E_{\text{high}} \gg E_{\text{low}}$  in the original theory, then by integrating the scale above  $E_{\text{high}}$ , an EFT with the energy scale  $E_{\text{low}}$  can be derived. The high energy contribution is to be incorporated in the effective couplings of the interactions in the EFT, which are referred to as the matching coefficients, at any desired fixed order of perturbation theory in the small ratio  $E_{\text{low}}/E_{\text{high}} \ll 1$ .

In the quarkonium system, it is considered that there exists a hierarchy of three types of energy scales,  $m \gg mv \gg mv^2$ , with a heavy quark mass  $m \gg \Lambda_{\text{QCD}}$  and a quark velocity  $v$ . NRQCD has been derived by integrating the energy scale above  $m$  in QCD, and pNRQCD by integrating further the energy scale above  $mv$  in NRQCD. Nonrelativistic nature of the quarkonium system then becomes manifest in these EFTs, and notably, a quantum mechanics-like hamiltonian emerges in pNRQCD. The matching coefficients in pNRQCD are dependent on the distance between a heavy quark and antiquark and eventually classified in powers of  $1/m$ . Thus a set of these matching coefficients can be regarded as *the heavy quark potential* consisting of a static potential and relativistic corrections. Therefore, once these matching coefficients are determined, various properties of quarkonia, such as the mass spectra, can be investigated systematically by solving the Schrödinger equation.

The nonperturbative matching is crucial for obtaining the heavy quark potential in pNRQCD as the energy scale of  $mv$  can be the same order of the magnitude as  $\Lambda_{\text{QCD}}$ . For this purpose, the present authors have been performing lattice QCD simulations and obtained accurate data so far up to the  $O(1/m^2)$  corrections [7, 8, 9, 10, 11]. The aim of the present report is then to demonstrate a spectroscopy analysis of quarkonia in pNRQCD with the lattice QCD results; the mass spectra of charmonium and bottomonium are computed by solving the Schrödinger equation, and the effect of relativistic corrections, in particular, the  $O(1/m)$  and the  $O(1/m^2)$  spin-orbit corrections are examined systematically. The pattern of the mass spectra is found to be in fairly good agreement with experimental data, in which the  $O(1/m)$  correction gives an important contribution.

## 2. pNRQCD and the heavy quark potential

We begin by describing how the hierarchy of energy scales in the heavy quarkonium system,  $m \gg mv \gg mv^2$ , is controlled along the derivation of NRQCD and pNRQCD and how the heavy

quark potential is defined nonperturbatively.

The first step is to integrate the energy scale above  $m$  in QCD, which leads to NRQCD. The meaning of the integration is that an interaction of heavy quarks via gluons whose momenta are larger than  $m$  is no more visible as a dynamical one and a creation or an annihilation of a heavy quark and antiquark pair cannot be seen within the resolution of the resulting obscured vacuum. Then, the heavy quark and antiquark are treated as independent external fields, respectively.

Let  $\psi$  and  $\chi_c$  be a quark and an antiquark annihilation operators, respectively, the NRQCD Lagrangian density with the leading interaction terms of the heavy quark and antiquark is written as [2, 3]

$$\begin{aligned} \mathcal{L}_{\text{NRQCD}} = & \psi^\dagger \left( iD_0 + \frac{\mathbf{D}^2}{2m} + \frac{\mathbf{D}^4}{8m^3} \right) \psi + (\psi \rightarrow \chi_c) - \frac{1}{4} F_{\mu\nu} F^{\mu\nu} \\ & + \psi^\dagger \left( c_F g \frac{\boldsymbol{\sigma} \cdot \mathbf{B}}{2m} + c_D g \frac{\mathbf{D} \cdot \mathbf{E} - \mathbf{E} \cdot \mathbf{D}}{8m^2} + i c_S g \frac{\boldsymbol{\sigma} \cdot (\mathbf{D} \times \mathbf{E} - \mathbf{E} \times \mathbf{D})}{8m^2} \right) \psi + (\psi \rightarrow \chi_c) \\ & + \frac{d_{ss}}{m^2} \psi^\dagger \psi \chi_c^\dagger \chi_c + \frac{d_{sv}}{m^2} \psi^\dagger \boldsymbol{\sigma} \psi \cdot \chi_c^\dagger \boldsymbol{\sigma} \chi_c + \frac{d_{vs}}{m^2} \psi^\dagger T^a \psi \chi_c^\dagger T^a \chi_c + \frac{d_{vv}}{m^2} \psi^\dagger T^a \boldsymbol{\sigma} \psi \cdot \chi_c^\dagger T^a \boldsymbol{\sigma} \chi_c, \quad (2.1) \end{aligned}$$

where  $\mathbf{B}$  and  $\mathbf{E}$  represent the color-magnetic and color-electric fields, and  $D_0$  and  $\mathbf{D}$  are the time and spatial components of covariant derivative. The Pauli matrix is denoted as  $\boldsymbol{\sigma}$ , and  $T^a$  ( $a = 1, \dots, 8$ ) are the SU(3) color generators. The factors  $c_F$ ,  $c_D$ ,  $c_S$ ,  $d_{ss}$ ,  $d_{sv}$ ,  $d_{vs}$ ,  $d_{vv}$  are the matching coefficients, which are to be determined so as to reproduce the same quantity, such as scattering amplitudes, both in QCD and NRQCD at any desired fixed order in perturbation theory of  $\alpha_s = g^2/(4\pi)$ . This matching is always performed perturbatively as  $m \gg \Lambda_{\text{QCD}}$ . In this way, the high energy momenta of gluons are integrated into the matching coefficients, while the remaining gluons in NRQCD carry nonrelativistic low energy momenta. For instance, if the matching scale is chosen just to be  $m$ , the matching coefficients of the bilinear term have the forms,  $c_F = 1 + \frac{\alpha_s}{2\pi} (C_F + C_A) + \mathcal{O}(\alpha_s^2)$ ,  $c_D = 1 + \frac{\alpha_s}{2\pi} C_A + \mathcal{O}(\alpha_s^2)$ ,  $c_S = 2c_F - 1$  [12], where  $C_F = 4/3$  and  $C_A = 3$  are the eigenvalues of the quadratic Casimir operators of the fundamental and adjoint representation in SU(3), respectively, and those of the four-Fermi contact terms are  $d_{ss} = \frac{2}{3}\pi\alpha_s + \mathcal{O}(\alpha_s^2)$ ,  $d_{sv} = -\frac{2}{9}\pi\alpha_s + \mathcal{O}(\alpha_s^2)$ ,  $d_{vs} = -\frac{1}{2}\pi\alpha_s + \mathcal{O}(\alpha_s^2)$ ,  $d_{vv} = \frac{1}{6}\pi\alpha_s + \mathcal{O}(\alpha_s^2)$  [13]. More general forms of the matching coefficients are provided in the original references [12, 13].

The second step is to integrate the energy scale above  $mv$  in NRQCD, which leads to pNRQCD. A merit of further integration is to avoid a complication due to a mixture of the remaining two energy scales  $mv$  and  $mv^2$  in NRQCD, which may affect a power counting of operators. The procedure is similar to the first step, i.e. one computes the same quantity in NRQCD and pNRQCD. However, in contrast to the first step, this matching must be performed nonperturbatively, since  $mv$  can be the same order of magnitude as  $\Lambda_{\text{QCD}}$ . The procedure proposed by Brambilla *et al.* [4, 5] for the nonperturbative matching is called the quantum mechanical matching, which consists of the following steps. Firstly one writes the NRQCD hamiltonian with the  $1/m$  expansion,  $H_{\text{NRQCD}} = H^{(0)} + \frac{1}{m}H^{(1)} + \frac{1}{m^2}H^{(2)} + \dots$  and then evaluates the expectation values of  $H^{(i \geq 1)}$  with an eigenstate of  $H^{(0)}$  projected onto a color-singlet  $q\bar{q}$  state. Typically, the expectation values of  $H^{(i \geq 1)}$  are represented with color-field strength correlators on the  $q\bar{q}$  source. Then, the ground state energies of these expectation values are compared to the pNRQCD matching coefficients, which are also

classified in powers of  $1/m$ ,

$$V_{\text{pNRQCD}} = V^{(0)} + \frac{1}{m}V^{(1)} + \frac{1}{m^2}V^{(2)} + \dots, \quad (2.2)$$

where  $V^{(i \geq 0)}$  are local in time but nonlocal in space (dependent on the  $q$ - $\bar{q}$  distance  $r$ ), hence they can be regarded as the components of the heavy quark potential.  $V^{(0)}$  is expressed with the Wilson loop, and thus, related to the static potential.  $V^{(i \geq 1)}$  are clearly due to finiteness of the quark mass, which are expressed with the color-field strength correlators and identified as the relativistic corrections to the static potential. So far these expressions are provided up to of  $O(1/m^2)$  [5, 6]. The second term in Eq. (2.2), corresponding to the  $O(1/m)$  correction, is expressed as [5]

$$V^{(1)}(r) = - \int dt t \langle\langle \mathbf{E}(0) \cdot \mathbf{E}(0) \rangle\rangle. \quad (2.3)$$

This term is typical in QCD due to the self interaction of gluons (three-gluon vertex). The double bracket  $\langle\langle \mathcal{O} \rangle\rangle$  indicates that an expectation value of an operator  $\mathcal{O}$  on a  $q$ - $\bar{q}$  source normalized by the expectation value of the  $q$ - $\bar{q}$  source itself. The third term contains the spin-dependent and spin-independent corrections. The spin-orbit correction in  $V^{(2)}$ , which is relevant in the following analysis, is expressed as [6]

$$V_{ls}^{(2)}(r) = \left( \frac{c_S}{2r} \frac{dV^{(0)}}{dr} + \frac{c_F}{r} \underbrace{(\varepsilon_{ijk} \hat{r}_i \int dt t \langle\langle \mathbf{B}^j(0) \mathbf{E}^k(0) \rangle\rangle)}_{\equiv V'_1(r)} + \varepsilon_{ijk} \hat{r}_i \underbrace{\int dt t \langle\langle \mathbf{B}^j(0) \mathbf{E}^k(r) \rangle\rangle}_{\equiv V'_2(r)} \right) \mathbf{l} \cdot \mathbf{s}. \quad (2.4)$$

The arguments of the color-field strength tensors in Eqs. (2.3) and (2.4), such as 0 or  $r$ , mean that a color-field strength tensor is attached to either quark or antiquark. The variable  $t$  is a relative temporal distance between the two color-field strength tensors, which is to be integrated. The matching coefficients  $V^{(i \geq 0)}(r)$  are then computed by lattice QCD simulations.

### 3. Brief summary of the lattice QCD results

The present authors have been studying the heavy quark potential in pNRQCD by using lattice QCD simulations within the quenched approximation [7, 8, 9, 10, 11]. The numerical procedure has been to use the Polyakov loop correlation function for the  $q$ - $\bar{q}$  source, and compute the field strength correlators by employing the multilevel algorithm, and evaluate them with transfer matrix theory. So far the potential with the  $O(1/m^2)$  relativistic corrections have been computed accurately up to the distance  $r \simeq 1$  fm.

Fig. 1 summarizes a part of the lattice QCD results which are relevant in the following spectrum analysis, the static potential, the  $O(1/m)$  correction, and the  $O(1/m^2)$  spin-orbit correction. The Sommer scale  $r_0 = 0.50$  fm has been used to fix the lattice spacing for each  $\beta$  value. The functional forms of the potentials from short to long distances have been determined by the following fitting functions,

$$V^{(0)}(r) = -\frac{\alpha}{r} + \sigma r + c^{(0)}, \quad (3.1)$$

$$V^{(1)}(r) = -\frac{9\alpha^2}{8r^2} + \sigma^{(1)} \ln r + c^{(1)}, \quad (3.2)$$

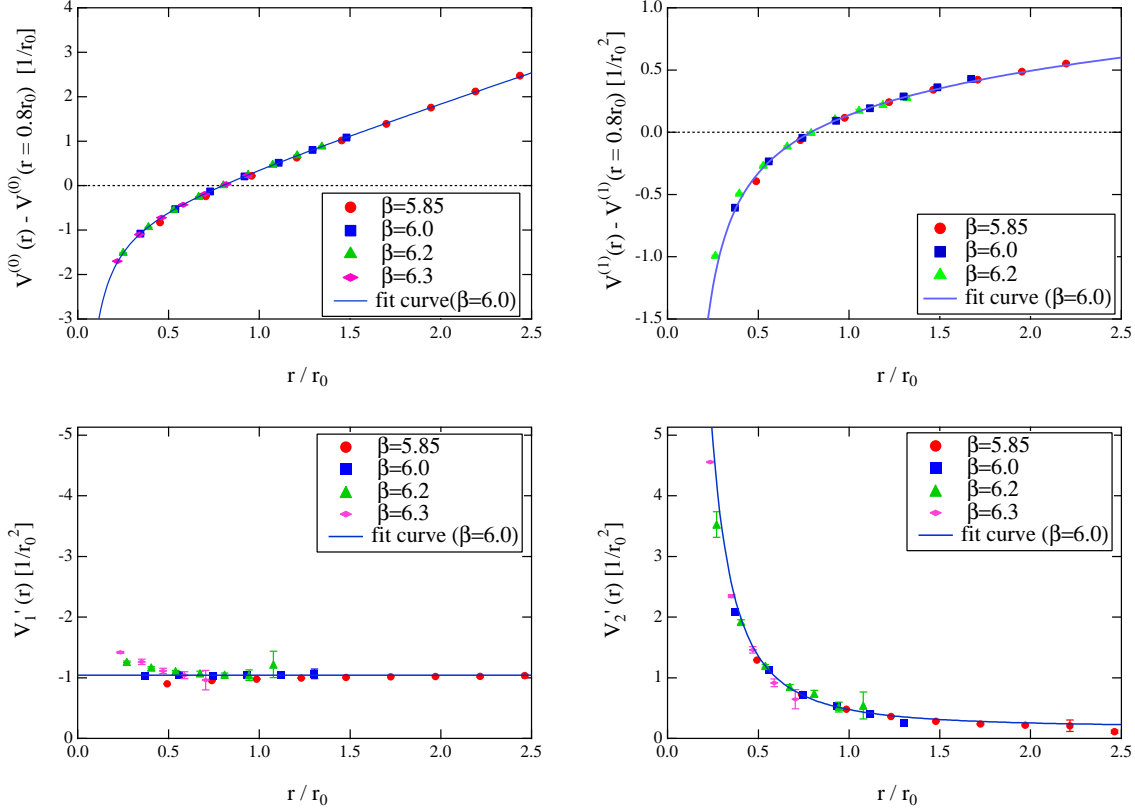


**Figure 1:** Summary of the lattice QCD results used in the present analysis, the static potential  $V^{(0)}$  (upper left), the  $O(1/m)$  correction  $V^{(1)}$  (upper right), and the  $O(1/m^2)$  spin-orbit corrections  $V'_1$  (lower left) and  $V'_2$  (lower right). Solid lines are the fitting curves.

$$V_{ls}^{(2)}(r) = \left( \frac{c_s}{2r} \frac{dV^{(0)}}{dr} + \frac{c_F}{r} (V'_1 + V'_2) \right) \mathbf{l} \cdot \mathbf{s}, \quad V'_1 = -(1-\varepsilon)\sigma, \quad V'_2 = \frac{\alpha}{r^2} + \varepsilon\sigma. \quad (3.3)$$

The fitting parameters have been found to be

$$\alpha = 0.297, \quad \sigma = 1.06 \text{ GeV/fm}, \quad \sigma^{(1)} = 0.142 \text{ GeV}^2, \quad \varepsilon = 0.2. \quad (3.4)$$

As can be seen in Fig. 1, the fitting curves nicely describe the behavior of the lattice data. Note that the leading order perturbation theory results in  $V^{(0)}(r) = -\frac{\alpha}{r}$  with  $\alpha \equiv C_F \alpha_s$ ,  $V^{(1)}(r) = -\frac{9\alpha^2}{8r^2}$ , and  $V'_1(r) = 0$ ,  $V'_2(r) = \alpha/r^2$ . The short distance behavior of  $V^{(0)}$ ,  $V^{(1)}$  and  $V'_2$  may follow these functions, although the coupling  $\alpha$  is different from the bare one. It can be observed that both  $V'_1$  and  $V'_2$  contain long-ranged nonperturbative tails, which are related to the string tension in  $V^{(0)}$  through the Gromes relation  $dV^{(0)}/dr = V'_2 - V'_1$  [14].

#### 4. Heavy quarkonium mass spectra in pNRQCD with the lattice QCD input

The Schrödinger equation

$$\left( 2m + \frac{\mathbf{p}^2}{m} + V^{(0)} \right) \psi^{(0)} = E^{(0)} \psi^{(0)} \quad (4.1)$$

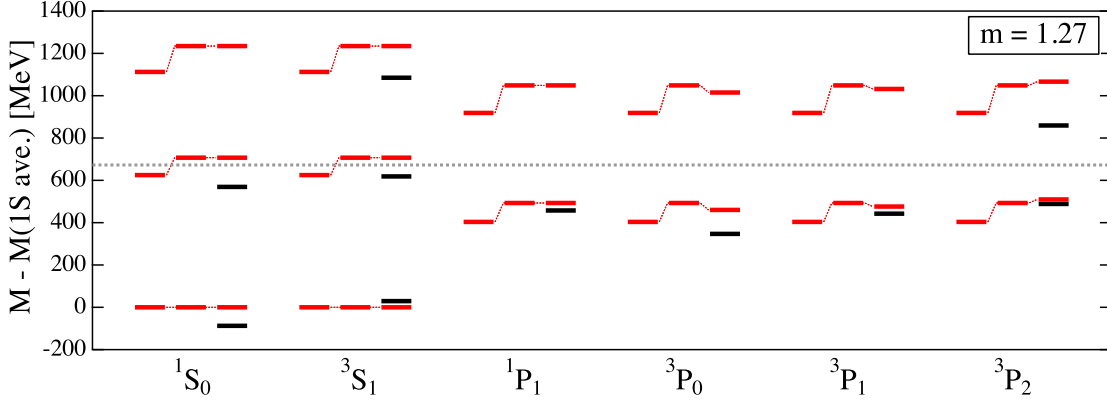


**Figure 2:** The mass spectra of charmonium for various quantum numbers,  $^{2S+1}L_J$ ; a set of three red lines in each state from left to right are the spectra of  $E^{(0)}$ ,  $E^{(0)} + \Delta E^{(1)}$ , and  $E^{(0)} + \Delta E^{(1)} + \Delta E_{ls}^{(2)}$ , respectively, while the black lines are the experimental data. The energy levels are normalized at the spin-averaged 1S state.

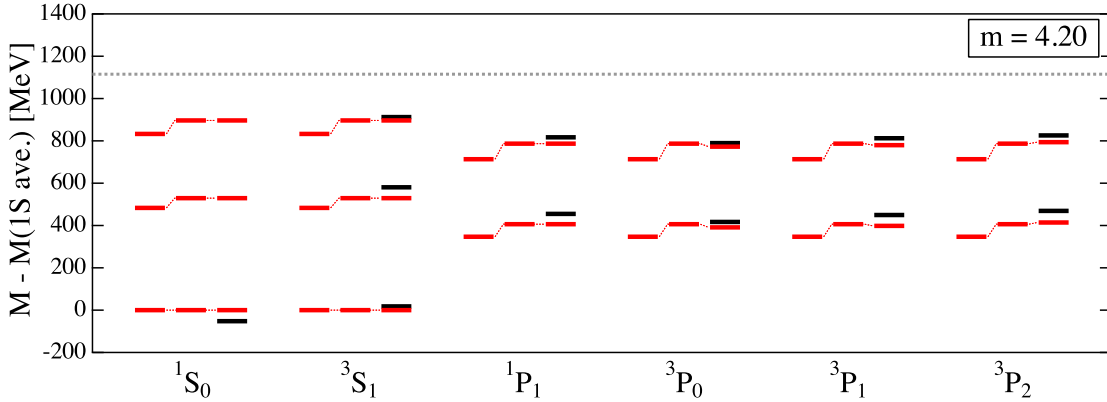


**Figure 3:** The same figure as Fig. 2, but for bottomonium.

is then solved and the energy  $E^{(0)}$  and the wave function  $\psi^{(0)}$  are computed. Using the wave function the corrections to  $E^{(0)}$  are evaluated in the first order perturbation theory,  $\Delta E^{(i)} = \langle \psi^{(0)} | V^{(i)} | \psi^{(0)} \rangle / m^i$  for  $i \geq 1$ . In this way, the heavy quarkonia of various quantum numbers are investigated systematically. The matching coefficients in NRQCD are dependent on the matching scale between QCD and NRQCD, and thus different for the charm and bottom quark sector, but they are simply assumed here to be the leading ones,  $c_F = c_S = 1$ , which correspond to taking the matching scale to be infinity. This issue will be discussed in the forthcoming paper. It should be emphasized that there is no free parameter except for the quark masses and a constant shift of the potential. The quark masses are chosen to be  $m_c = 1.27$  GeV (charm) and  $m_b = 4.20$  GeV (bottom) in this analysis.

Figs. 2 and 3 show the mass spectra of charmonium and bottomonium, respectively, for various quantum numbers classified by  $^{2S+1}L_J$ . The energy levels are normalized at the spin-averaged 1S state. A fairly good agreement can be observed between the computed pattern of the mass spectra

and the experimental data, especially for the states below the  $D\bar{D}$  threshold for charmonium and the  $B\bar{B}$  threshold for bottomonium, in which the effect of the  $O(1/m)$  correction is remarkable. As is clear from the  $\mathbf{l}\cdot\mathbf{s}$  operator, the  $O(1/m^2)$  spin-orbit correction affects the splitting among the levels of  ${}^3P_{J=0,1,2}$  states, the fine splitting, where  $\langle {}^3P_J|\mathbf{l}\cdot\mathbf{s}|{}^3P_J\rangle = -2, -1, 1$  for  $J = 0, 1, 2$ , respectively. The splitting is less noticeable than that caused by the  $O(1/m)$  correction as the matching scale effect of QCD and NRQCD is not yet properly taken into account. The experimental level order of  ${}^3P_J$  states exhibits  $\Delta E({}^3P_1 - {}^3P_0) > \Delta E({}^3P_2 - {}^3P_1)$ , but if only the spin-orbit interaction contributes, this will be opposite regardless the functional form of the spin-orbit correction due to the factor of  $\langle {}^3P_J|\mathbf{l}\cdot\mathbf{s}|{}^3P_J\rangle$ . It would be crucial to take into account the spin-tensor contribution.

## 5. Summary

We have studied the charmonium and bottomonium mass spectra in potential nonrelativistic QCD (pNRQCD) with the lattice QCD results of the heavy quark potential. In pNRQCD, the heavy quark potential consists of a static potential and relativistic corrections classified in powers of  $1/m$ , and in the present investigation, we have examined the effect of the  $O(1/m)$  correction and the  $O(1/m^2)$  spin-orbit correction systematically. We have found that the pattern of the mass spectra is in fairly good agreement with the experimental data, in which the  $O(1/m)$  correction gives an important contribution. This effect has not been taken into account in the conventional phenomenological models. It is certainly interesting to see all the effect up to the  $O(1/m^2)$  correction in pNRQCD on the spectra, which contain the velocity-dependent potentials as well as the other types of the spin-dependent corrections.

## References

- [1] J. Beringer *et al.* (Particle Data Group), *Phys.Rev.* **D86** (2012) 010001.
- [2] W. Caswell and G. Lepage, *Phys.Lett.* **B167** (1986) 437.
- [3] G. T. Bodwin, E. Braaten and G. P. Lepage, *Phys.Rev.* **D51** (1995) 1125–1171 [hep-ph/9407339].
- [4] N. Brambilla, A. Pineda, J. Soto, and A. Vairo, *Rev.Mod.Phys.* **77** (2005) 1423 [hep-ph/0410047].
- [5] N. Brambilla, A. Pineda, J. Soto, and A. Vairo, *Phys. Rev.* **D63** (2001) 014023 [hep-ph/0002250].
- [6] A. Pineda and A. Vairo, *Phys.Rev.* **D63** (2001) 054007 [hep-ph/0009145].
- [7] M. Koma, Y. Koma, and H. Wittig, *PoS LAT2005* (2006) 216 [hep-lat/0510059].
- [8] Y. Koma, M. Koma, and H. Wittig, *Phys.Rev.Lett.* **97** (2006) 122003 [hep-lat/0607009].
- [9] Y. Koma and M. Koma, *Nucl.Phys.* **B769** (2007) 79–107 [hep-lat/0609078].
- [10] Y. Koma and M. Koma, *PoS LAT2009* (2009) 122 [arXiv:0911.3204].
- [11] Y. Koma and M. Koma, *Prog.Theor.Phys.Suppl.* **186** (2010) 205–210.
- [12] A. V. Manohar, *Phys.Rev.* **D56** (1997) 230–237 [hep-ph/9701294].
- [13] A. Pineda and J. Soto, *Phys.Rev.* **D58** (1998) 114011 [hep-ph/9802365].
- [14] D. Gromes, *Z.Phys.* **C26** (1984) 401.